Evidence of nighttime production of organic nitrates during SEAC^{4}RS, FRAPPÉ, and KORUS-AQ

Hannah S. Kenagy[1], Tamara L. Sparks[1], Paul J. Wooldridge[1], Andrew J. Weinheimer[2], Thomas B. Ryerson[3], Donald R. Blake[4], Eric C. Apel[2], and Ronald C. Cohen[1,5]

[1]Department of Chemistry, University of California, Berkeley, CA, USA
[2]Atmospheric Chemistry Observations and Modeling, National Center for Atmospheric Research, Boulder, CO, USA
[3]Chemical Sciences Division, NOAA Earth System Research Laboratory, Boulder, CO, USA
[4]Department of Chemistry, University of California, Irvine, CA, USA
[5]Department of Earth and Planetary Science, University of California, Berkeley, CA, USA

Key Points:

- Evidence for nocturnal NO_3-initiated production of organic nitrates similar in magnitude to daytime OH-initiated production
- Significant nocturnal production of organic nitrates observed from three aircraft-based field campaigns in chemically-distinct environments
- Nighttime production of organic nitrates impacts our understanding of the nighttime lifetime and fate of NOx

Corresponding author: Ronald C. Cohen, rccohen@berkeley.edu

Abstract

Organic nitrates ($RONO_2$) are an important NO_x sink. In rural environments dominated by biogenic emissions, nocturnal NO_3-initiated production of $RONO_2$ is competitive with daytime OH-initiated $RONO_2$ production. However, in urban areas, OH-initiated production of $RONO_2$ has been assumed dominant and NO_3-initiated production considered negligible. We show evidence for nighttime $RONO_2$ production similar in magnitude to daytime production during three aircraft campaigns in chemically-distinct environments: SEAC^{4}RS in the rural Southeastern US, FRAPPÉ in the Colorado Front Range, and KORUS-AQ around the megacity of Seoul. During each campaign, morning observations show $RONO_2$ enhancements at constant, near-background O_x ($\equiv O_3 + NO_2$), indicating that the $RONO_2$ are from a non-photochemical source, whereas afternoon observations show a strong correlation between $RONO_2$ and O_x resulting from photochemical production. We show there are sufficient precursors for nighttime $RONO_2$ formation during all three campaigns. This evidence impacts our understanding of the nighttime lifetime and fate of NO_x.

Plain Language Summary

Nitrogen oxides are pollutants emitted during combustion which are involved in ozone and secondary organic aerosol production. One way in which nitrogen oxides are removed from the atmosphere is via chemistry that converts them to organic nitrates. This conversion of nitrogen oxides to organic nitrates has been thought to occur primarily during the day when the chemistry is driven by sunlight. Here we show evidence that nighttime processes generate similar quantities of organic nitrates to those produced by sunlight-driven processes.

1 Introduction

Nitrogen oxides (NO_x=$NO + NO_2$) are important tropospheric oxidants that contribute to ozone (O_3) formation, secondary organic aerosol production, and nitrogen deposition to ecosystems. Alkyl and multifunctional nitrates ($RONO_2$) are an oxidative sink of NO_x. Previous studies have shown that $RONO_2$ production is a significant NO_x loss pathway (Day et al., 2003), especially as urban NO_x concentrations decrease (Perring et al., 2013; Romer Present et al., 2019). Organic nitrates can be generated through both daytime photochemical oxidation pathways initiated by OH and nighttime oxidation pathways initiated by NO_3.

During the day, $RONO_2$ is produced photochemically as a radical termination step in a series of reactions between oxidized VOCs (volatile organic compounds) and NO_x (shown in Figure 1). VOCs are oxidized by OH to form organic peroxy radicals, RO_2 (R1). Reaction between NO and organic peroxy radicals can result in formation of an organic nitrate (R2, minor pathway, branching ratio α). The major pathway for the reaction between RO_2 and NO (R3), however, continues radical propagation to form two ozone molecules (R4, R5, R6). Consequently, this daytime chemistry produces both O_x ($\equiv O_3 + NO_2$) and $RONO_2$ so, if photochemistry is dominant, we expect a correlation between O_x and $RONO_2$. Typically, chain lengths are such that we expect 6-20 O_x for each $RONO_2$.

$$\mathrm{RH + OH \longrightarrow RO_2 + H_2O} \quad \text{(R1)}$$
$$\mathrm{RO_2 + NO \longrightarrow RONO_2} \quad \text{(R2)}$$
$$\mathrm{RO_2 + NO \longrightarrow RO + NO_2} \quad \text{(R3)}$$
$$\mathrm{RO + O_2 \longrightarrow R'(O) + HO_2} \quad \text{(R4)}$$
$$\mathrm{HO_2 + NO \longrightarrow OH + NO_2} \quad \text{(R5)}$$
$$\mathrm{2\,NO_2 + h\nu \longrightarrow 2\,O(^3P) \longrightarrow 2\,O_3} \quad \text{(R6)}$$
$$\text{(R7)}$$

At night, $RONO_2$ is produced from alkenes via addition of NO_3 to a double bond (R10), as shown in Figure 1. NO_3 is formed from reaction between NO_2 and O_3 (R9). During the day, NO_3 is quickly photolyzed, but at night, NO_3 concentrations can build up and react with alkenes. Two O_3 molecules are consumed in the production of NO_3 (R8 followed by R9), meaning that nighttime $RONO_2$ formation is a net sink of O_x. Consequently, we do not expect a positive correlation between $RONO_2$ and O_x if NO_3 is the dominant oxidant, and we might even expect a weak negative correlation.

$$\mathrm{NO + O_3 \longrightarrow NO_2} \quad \text{(R8)}$$
$$\mathrm{NO_2 + O_3 \longrightarrow NO_3 + O_2} \quad \text{(R9)}$$
$$\mathrm{NO_3 + R_1{=}R_2 \longrightarrow R_2(ONO_2){-}R_2} \quad \text{(R10)}$$

The fate of NO_x at night is controlled by the balance of two NO_3 reaction pathways. First, NO_x can be lost via NO_3 reaction with alkenes, as described above. Second, NO_3 can be lost at night via reaction with NO_2 to form N_2O_5 in thermal equilibrium, followed by aerosol uptake and heterogeneous hydrolysis to produce HNO_3 and, to a smaller degree, $ClNO_2$. The competition between these two pathways is controlled by both the availability of alkenes and by the fate of N_2O_5. Nighttime $RONO_2$ production increases in environments with high biogenic alkene emissions (isoprene, monoterpenes) and in environments with high anthropogenic alkene emissions, particularly where either of these two emission sources is sustained overnight. The N_2O_5 to HNO_3 pathway becomes less competitive with $RONO_2$ formation in environments with low aerosol surface area and small heterogeneous uptake coefficients for N_2O_5 ($\gamma(N_2O_5)$), as these decrease the rate of heterogeneous hydrolysis of N_2O_5 to HNO_3. Additionally, higher temperatures shift the N_2O_5 equilibrium towards dissociation, making N_2O_5 formation less favorable, while also increasing the rate of bimolecular NO_3 reactions with alkenes. Thus, nighttime $RONO_2$ formation is most favorable in environments with high alkene emissions, low aerosol surface area, small $\gamma(N_2O_5)$, and high temperatures.

There is reason to suspect that $RONO_2$ production from nighttime NO_3 oxidation of VOCs could be competitive with $RONO_2$ production from photochemical OH oxidation. A shallow planetary boundary layer characteristic of many nighttime environments results in increased concentrations. Higher concentrations of precursors increases the rate of bimolecular reactions, thereby increasing the rate of formation of NO_3 and the reaction of NO_3 with alkenes. Moreover, $RONO_2$ yields from NO_3-initiated oxidation (20-80%) are far larger than $RONO_2$ yields from OH-initiated oxidation of VOCs (0.1-35%). Even if NO_3 oxidation represents a smaller fraction of total VOC oxidation than OH oxidation, the larger $RONO_2$ yields could make $RONO_2$ production from NO_3 oxidation competitive with $RONO_2$ production from OH oxidation.

A number of recent studies have shown that NO_3 oxidation can be a significant source of $RONO_2$ in regions dominated by biogenic VOC emissions. In forested regions of Col-

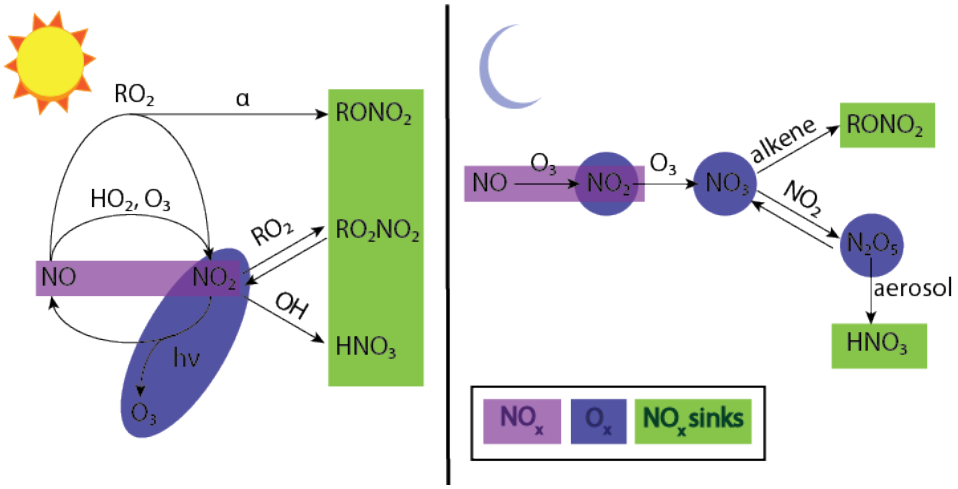

Figure 1. Schematic of daytime (left) and nighttime (right) NO_x chemistry.

orado, Finland, and Germany, nighttime production of $RONO_2$ was found to be comparable to daytime $RONO_2$ (Fry et al., 2013; Sobanski et al., 2016; Liebmann et al., 2019). Other studies have found NO_3-initiated formation of isoprene nitrates to be competitive with OH-initiated formation of isoprene nitrates in the Southeastern United States (Starn et al., 1998; Xiong et al., 2015), in an observationally-constrained model of the the eastern United States (Horowitz et al., 2007), and in a global model (von Kuhlmann et al., 2003).

Moreover, NO_3 oxidation has been shown to be a significant source of organic aerosol in in the Central Valley of California (Rollins et al., 2012), the Southeastern United States (Ayres et al., 2015; B. H. Lee et al., 2016; Xu, Guo, et al., 2015; Xu, Suresh, et al., 2015; Pye et al., 2015; Fisher et al., 2016), in a forested region of Colorado (Fry et al., 2013), in rural Southwestern Germany (Huang et al., 2019), throughout Europe (Kiendler-Scharr et al., 2016), and in the Alberta oil sands (A. K. Y. Lee et al., 2019).

Though NO_3 chemistry has been shown to be an important source of $RONO_2$ and secondary organic aerosol in rural regions dominated by biogenic emissions, nocturnal NO_3-initiated $RONO_2$ formation has often been considered negligible in comparison to daytime OH-initiated production of $RONO_2$ in urban environments. In this study, we present evidence for significant nighttime $RONO_2$ production using measurements of O_x and $RONO_2$ from three aircraft-based field campaigns in distinct environments. First, we show evidence for significant nighttime $RONO_2$ production in the rural southeastern United States during SEAC^{4}RS, an area with high biogenic emissions. Second, we show similarly high nighttime $RONO_2$ production in two urban areas: in the Colorado Front Range during FRAPPÉ, which is affected by both high urban and oil/gas emissions, as well as in and around the megacity of Seoul during KORUS-AQ. In each location, we show that the expected linear relationship between O_x and $RONO_2$ is observed during the afternoon. However, during the morning hours, the relationship between O_x and $RONO_2$ shows evidence of nighttime $RONO_2$ production. We support this conclusion further by assessing precursor availability for nighttime $RONO_2$ production.

2 Measurements

2.1 SEAC^{4}RS, FRAPPÉ, and KORUS-AQ aircraft campaigns

The Studies of Emissions and Atmospheric Composition, Clouds, and Climate Coupling by Regional Surveys (SEAC^{4}RS) campaign took place during August-September 2013 in the Southeastern and Western US. This analysis uses observations from the NASA DC-8 aircraft which flew 19 research flights out of Ellington Field, near Houston, TX.

The Front Range Air Pollution and Photochemistry Experiment (FRAPPÉ) took place during July - August 2014 in the Northern Front Range Metropolitan Area (NFRMA) of Colorado. This analysis uses observations from the NSF/NCAR C-130 aircraft which flew fifteen daytime research flights out of the Rocky Mountain Metropolitan Airport in Jefferson County, CO.

The Korea-United States Air Quality Study (KORUS-AQ) campaign took place during May and June 2016 over South Korea and the Yellow Sea. This analysis uses observations from the NASA DC-8 aircraft which flew 20 daytime research flights out of Pyeongtaek, South Korea ($\approx$ 60 km south of Seoul).

2.2 Instrumentation

During all three campaigns, measurements of NO_2 and $RONO_2$ were made by the UC Berkeley thermal dissociation laser induced fluorescence (TD-LIF) instrument (Day et al., 2002). Briefly, one channel of the instrument measures NO_2 by laser induced fluorescence. Two other channels first flow air through a heated quartz oven. One channel is set at 180 °C, the temperature at which peroxy nitrates (RO_2NO_2) dissociate into RO_2 and NO_2. The second is set at 360 °C, the temperature at which $RONO_2$ dissociate into RO + NO_2. The difference in NO_2 detected in adjacent channels gives the mixing ratio for each class of compounds: the RO_2NO_2 mixing ratio is the difference between the 180 °C channel and the unheated channel, and the $RONO_2$ mixing ratio is the difference between the 360 °C channel and the 180 °C channel.

O_3 and NO were measured by chemiluminescence. During SEAC^{4}RS, O_3 and NO were measured by the NOAA NO_yO_3 instrument (Ryerson et al., 2000). During FRAPPÉ and KORUS-AQ, O_3 and NO were measured by the NCAR chemiluminescence instrument (Ridley et al., 1994).

Alkenes were measured by whole air sampling (WAS) and trace organic gas analyzer (TOGA). For SEAC^{4}RS and KORUS-AQ, we use WAS measurements of propene, butene, isoprene, α-pinene, and β-pinene. During FRAPPÉ, we use WAS measurements of propene, isoprene, α-pinene, and β-pinene and TOGA measurements of butene and limonene.

3 Observations/Results

3.1 O_x versus $RONO_2$

The relationship between O_x and $RONO_2$ during each campaign is shown in Figure 2. During all three campaigns, during the afternoon hours (13:00 - 19:00), there is a positive, linear relationship between O_x and $RONO_2$, indicating that photochemical production of both O_x and $RONO_2$ is occurring. The slope of the relationship between O_x and $RONO_2$ mixing ratios is indicative of the branching ratio between O_x and $RONO_2$ production. From Figure 2, during SEAC^{4}RS, 29 O_x are produced for each $RONO_2$. Chain lengths are shorter during FRAPPÉ, where 12 O_x are produced for each $RONO_2$, and longer during KORUS-AQ, where 43 O_x are produced for each $RONO_2$.

	SEAC^{4}RS	FRAPPÉ	KORUS-AQ
$RONO_2$ (ppt)	120	980	560
propene (ppt)	N/A	84	88
butene (ppt)	N/A	26	58
isoprene (ppt)	N/A	130	61
α-pinene (ppt)	N/A	N/A	16
β-pinene (ppt)	N/A	N/A	13
limonene (ppt)	N/A	6.8	N/A
$\Sigma_i \alpha_i [VOC]_i$ (ppt)	N/A	160	140
NO_x (ppb)	0.43	3.5	6.5

Table 1. Table of the average $RONO_2$, alkene, and NO_x concentrations in morning (before 10:00). Nitrate yields used are from (Perring et al., 2013) and references therein. There are insufficient morning SEAC^{4}RS measurements to report meaningful average alkene mixing ratios.

During the morning hours (before 11:00), however, the relationship between O_x mixing ratios and $RONO_2$ mixing ratios has a flat (zero) slope. At a relatively constant observed O_x mixing ratio, a wide range of $RONO_2$ mixing ratios were observed. This indicates that O_x and $RONO_2$ are not produced from the same pathway. Instead, the high levels of $RONO_2$ at relatively low levels of O_x suggest that many of the observed $RONO_2$ were produced via a non-photochemical pathway that produces $RONO_2$ without generating O_x. Since this trend is only observed in the morning, and not in the afternoon, it is indicative of a large source of $RONO_2$ produced from NO_3 oxidation overnight. We also explored the effects of O_3 deposition and nighttime dynamics, but neither could sufficiently explain the observed trend.

3.2 Precursors for nighttime $RONO_2$ production

As additional evidence for nighttime $RONO_2$ production, we assess the availability of precursors to $RONO_2$ production, namely NO_3 and alkenes. We tabulate average morning mixing ratios of $RONO_2$, alkenes, and NO_x in Table 1. The abundance of NO_x and alkenes observed in the morning indicates that these precursors are not depleted by overnight chemistry; rather, the non-zero concentrations of precursors in the morning suggests that NO_3-initiated $RONO_2$ production chemistry is sustained overnight and occurs until daybreak.

During SEAC^{4}RS, there were insufficient morning alkene measurements to report meaningful averages. However, average diurnal profiles of monoterpenes (not shown) over the southeast US during the Southern Oxidant and Aerosol Study (SOAS) show that the mixing ratios of α-pinene and β-pinene both increase overnight, evidence that there is monoterpene emission overnight which occurs faster than loss to $RONO_2$ production. Therefore, there is an abundance of alkenes available overnight to form alkyl nitrates.

4 Discussion and Conclusion

We show evidence of significant nighttime $RONO_2$ production during three aircraft campaigns in three distinct locations: the rural southeastern United States dominated by biogenic emissions (SEAC^{4}RS), the Colorado Front Range dominated by a combination of urban and oil/gas emissions (FRAPPÉ), and the megacity of Seoul dominated by urban emissions (KORUS-AQ). Though, in urban areas, nighttime production of $RONO_2$ has often been considered negligible in comparison to daytime production, we show ev-

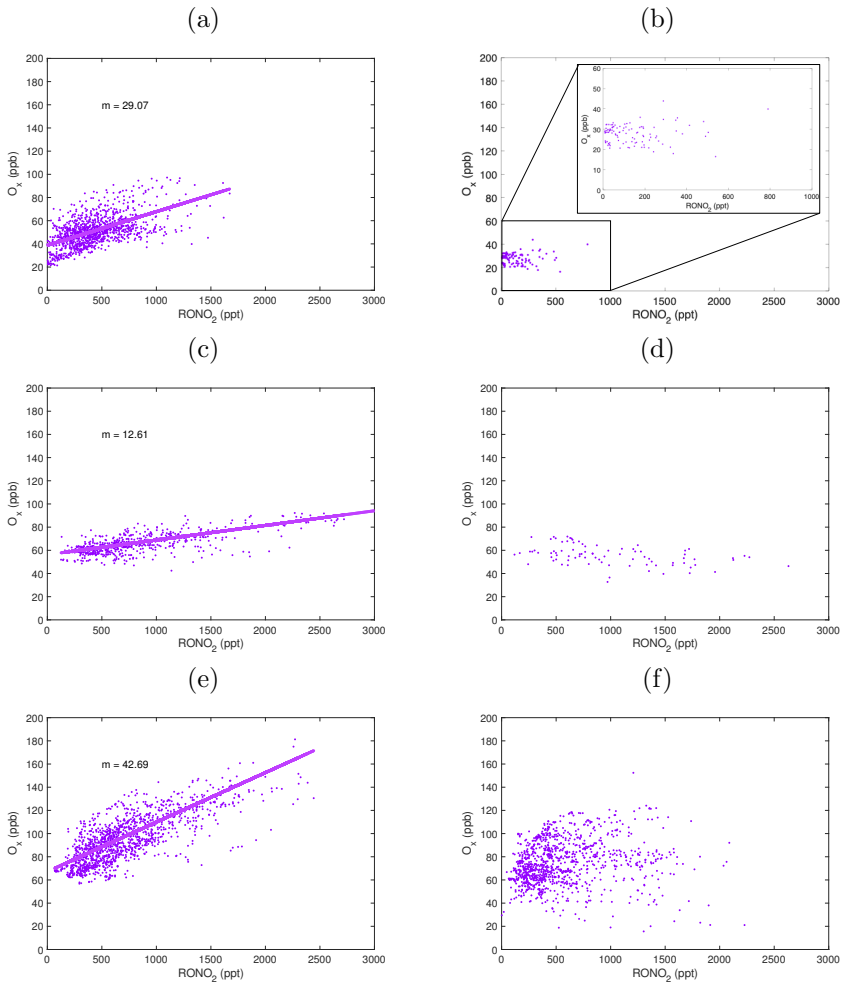

Figure 2. Plots of O_x vs. $RONO_2$ during SEAC^{4}RS (a, b), FRAPPÉ (c,d) and KORUS-AQ (e,f) during afternoon (left: a, c, e) and morning (right: b, d, f). Only data in the boundary layer ($<$ 1 km for SEAC^{4}RS and KORUS-AQ, $<$ 2 km for FRAPPÉ) are included. York linear fits (with slopes labeled as m) to the afternoon data are shown.

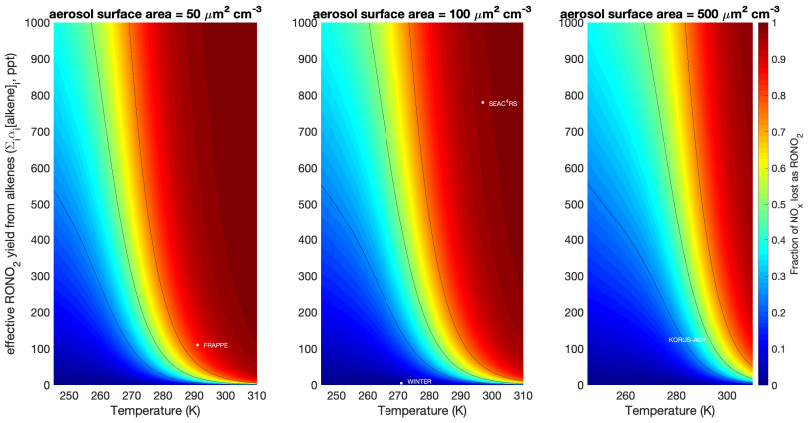

Figure 3. Fraction of NO_x lost as $RONO_2$, shown as a function of temperature and effective $RONO_2$ yield from alkenes ($\Sigma_i \alpha_i [\text{alkene}]_i$) for three different aerosol surface areas (50, 100, and 500 $\mu m^2\,cm^{-3}$). We assume 1 ppb NO_2, 40 ppb O_3, 1013 hPa, $\gamma_{N2O5} = 0.04$, and NO_3 and N_2O_5 in steady-state. Black contour lines correspond to 25%, 50% and 75% of NO_x lost as $RONO_2$. Average conditions during SEAC^{4}RS, FRAPPÉ, and KORUS-AQ are shown. Average conditions during WINTER (NSF aircraft campaign over Northeastern US during Feb-Mar 2015) are also shown as an example of conditions during which HNO_3 is the dominant nighttime sink of NO_x ((Kenagy et al., 2018)).

idence for nighttime $RONO_2$ production that results in morning $RONO_2$ mixing ratios of similar magnitude to afternoon observations of $RONO_2$ in all three of these distinct environments.

Rapid nighttime $RONO_2$ production impacts our understanding of the lifetime and fate of NO_x at night. Evidence for nighttime $RONO_2$ production indicates that HNO_3 produced via heterogeneous hydrolysis of N_2O_5 is not necessarily the dominant nighttime sink of NO_x. In environments with low aerosol loading, high temperatures, and an abundance of alkenes, $RONO_2$ production can be the dominant nighttime NO_x sink. Significant nocturnal NO_3-initiated $RONO_2$ production in urban areas also has implications for substantial overnight secondary organic aerosol production in and around cities.

We explore the effects of temperature, alkenes, and aerosol surface area on the fraction of NO_x lost as $RONO_2$ at night in Figure 3, assuming constant NO_2, O_3, pressure, and γ_{N2O5}, and NO_3 and N_2O_5 in steady-state (see Appendix A). Under these model conditions, the temperature, alkenes, and aerosol surface area during FRAPPÉ and SEAC^{4}RS indicate that $RONO_2$ is the dominant sink of NO_x at night, and during KORUS-AQ indicate that overnight NO_x loss is evenly split between HNO_3 and $RONO_2$. For contrast, during the WINTER campaign (aircraft campaign over NE US, Feb-Mar 2015), low temperatures and low alkene concentrations lead to HNO_3-dominant NO_x loss at night (Kenagy et al., 2018).

Here we have presented evidence for a significant, and sometimes dominant, nighttime source of $RONO_2$ using airborne, daytime measurements. Stationary measurements of the full diel variations in $RONO_2$ and its precursors in cities would help further elucidate the relative importance of the different mechanisms for $RONO_2$ formation. Additionally, measurements of the diel cycle of $RONO_2$ could provide insights into the fate of daytime- and nighttime-produced $RONO_2$ by showing whether they remain in the gas

phase or partition into particles and whether hydrolysis, oxidation, or deposition dominates loss of $RONO_2$.

Appendix A Calculating fraction of NO_x lost as $RONO_2$ overnight

We calculate the nighttime production of $RONO_2$ from reaction of NO_3 and alkenes (R10) and the nighttime production of HNO_3 from heterogeneous hydrolysis of N_2O_5 as:

$$P(\mathrm{RONO_2}) = \alpha \times k_{\mathrm{NO_3\ +\ alkene}} \times [\mathrm{alkenes}] \times [\mathrm{NO_3}] \tag{A1}$$

$$P(\mathrm{HNO_3}) = k_{hyd}[\mathrm{N_2O_5}],\ \text{where } k_{hyd} = \frac{1}{4} \times \bar{c}_{\mathrm{N_2O_5}} \times \mathrm{SA} \times \gamma_{N_2O_5} \tag{A2}$$

Here α is the branching ratio for $RONO_2$ production from the reaction of NO_3 with alkenes, $\bar{c}_{\mathrm{N_2O_5}}$ represents the mean molecular speed of N_2O_5, $\gamma_{N_2O_5}$ represents the heterogeneous uptake coefficient for N_2O_5, and SA represents the aerosol surface area per volume of air.

We use the rate constant for the reaction of NO_3 + isoprene for $k_{\mathrm{NO_3\ +\ alkene}}$. Values for $k_{\mathrm{NO_3\ +\ alkene}}$ and for k_b are from the IUPAC chemical kinetics database (Atkinson et al., 2004, 2006). Values for $k_{\mathrm{NO_2\ +\ O_3}}$ and for k_f are from JPL Data Evaluation #18 (Burkholder et al., 2015). We assume constant NO_2 (1 ppb), O_3 (40 ppb), pressure (1013 hPa), and γ_{N2O5} (0.04). Additionally, we assume NO_3 and N_2O_5 in steady-state:

$$[\mathrm{NO_3}]_{SS} = \frac{k_{\mathrm{NO_2\ +\ O_3}}[\mathrm{NO_2}][\mathrm{O_3}]}{k_{\mathrm{NO_3\ +\ alkene}}[\mathrm{alkene}]} \tag{A3}$$

$$[\mathrm{N_2O_5}]_{SS} = \frac{k_f[\mathrm{NO_3}][\mathrm{NO_2}]}{k_b + k_{hyd}} \tag{A4}$$

where k_f represents the formation of N_2O_5 from NO_2 and NO_3 and k_b represents the decomposition of N_2O_5 into NO_2 and NO_3.

Acknowledgments

This work was supported by NASA grant 80NSSC18K0624 and an NSF Graduate Research Fellowship to H.S.K. (DGE1106400). We thank the science teams of SEAC^{4}RS, FRAPPÉ, and KORUS-AQ. Data from SEAC^{4}RS are available at `https://www-air.larc.nasa.gov/cgi-bin/ArcView/seac4rs`. Data from FRAPPÉ are available at `https://data.eol.ucar.edu/master_lists/generated/frappe/`. Data from KORUS-AQ are available at `https://www-air.larc.nasa.gov/cgi-bin/ArcView/korusaq?DC8=1`.

References

Atkinson, R., Baulch, D. L., Cox, R. A., Crowley, J. N., Hampson, R. F., Hynes, R. G., ... Troe, J. (2004). Evaluated kinetic and photochemical data for atmospheric chemistry: Volume I - gas phase reactions of O_{x}, HO_{x}, NO_{x} and SO_{x} species. *Atmos. Chem. Phys.*, *4*(6), 1461–1738. Retrieved from `http://www.atmos-chem-phys.net/4/1461/2004/` doi: 10.5194/acp-4-1461-2004

Atkinson, R., Baulch, D. L., Cox, R. A., Crowley, J. N., Hampson, R. F., Hynes, R. G., ... IUPAC Subcommittee (2006). Evaluated kinetic and photochemical data for atmospheric chemistry: Volume II - gas phase reactions of organic species. *Atmos. Chem. Phys.*, *6*(11), 3625–4055. Retrieved from `http://www.atmos-chem-phys.net/6/3625/2006/` doi: 10.5194/acp-6-3625-2006

Ayres, B. R., Allen, H. M., Draper, D. C., Brown, S. S., Wild, R. J., Jimenez, J. L., ... Fry, J. L. (2015). Organic nitrate aerosol formation via NO3+ biogenic volatile organic compounds in the southeastern United States. *Atmos. Chem. Phys.*, *15*(23), 13377–13392. doi: 10.5194/acp-15-13377-2015

Burkholder, J. B., Sander, S. P., Abbatt, J. P. D., Barker, J. R., Huie, R. E., Kolb, C. E., ... Wine, P. H. (2015). *Chemical Kinetics and Photochemical Data for Use in Atmospheric Studies, Evaluation No. 18* (Tech. Rep.). Pasadena: Jet Propulsion Laboratory. Retrieved from `https://jpldataeval.jpl.nasa.gov`

Day, D. A., Dillon, M. B., Wooldridge, P. J., Thornton, J. A., Rosen, R. S., Wood, E. C., & Cohen, R. C. (2003). On alkyl nitrates, O₃, and the “missing NO_y”. *J. Geophys. Res.*, *108*(D16), JD003685. Retrieved from `http://doi.wiley.com/10.1029/2003JD003685` doi: 10.1029/2003JD003685

Day, D. A., Wooldridge, P. J., Dillon, M. B., Thornton, J. A., & Cohen, R. C. (2002, mar). A thermal dissociation laser-induced fluorescence instrument for in situ detection of NO2 , peroxy nitrates, alkyl nitrates, and HNO3. *J. Geophys. Res. Atmos.*, *107*(D6), ACH 4–1–ACH 4–14. Retrieved from `http://doi.wiley.com/10.1029/2001JD000779` doi: 10.1029/2001JD000779

Fisher, J. A., Jacob, D. J., Travis, K. R., Kim, P. S., Marais, E. A., Chan, C., ... Day, D. A. (2016). Organic nitrate chemistry and its implications for nitrogen budgets in an isoprene- and monoterpene-rich atmosphere : constraints from aircraft (SEAC 4 RS) and ground-based (SOAS) observations in the Southeast US. *Atmos. Chem. Phys.*, *16*, 5969–5991. doi: 10.5194/acp-16-5969-2016

Fry, J. L., Draper, D. C., Zarzana, K. J., Campuzano-Jost, P., Day, D. A., Jimenez, J. L., ... Grossberg, N. (2013). Observations of gas- and aerosol-phase organic nitrates at BEACHON-RoMBAS 2011. *Atmos. Chem. Phys.*, *13*(17), 8585–8605. doi: 10.5194/acp-13-8585-2013

Horowitz, L. W., Fiore, A. M., Milly, G. P., Cohen, R. C., Perring, A., Wooldridge, P. J., ... Lamarque, J. F. (2007). Observational constraints on the chemistry of isoprene nitrates over the eastern United States. *J. Geophys. Res. Atmos.*, *112*(12), 1–13. doi: 10.1029/2006JD007747

Huang, W., Saathoff, H., Shen, X., Ramisetty, R., Leisner, T., & Mohr, C. (2019). Chemical Characterization of Highly Functionalized Organonitrates Contributing to Night-Time Organic Aerosol Mass Loadings and Particle Growth. *Environ. Sci. Technol.*, *53*(3), 1165–1174. doi: 10.1021/acs.est.8b05826

Kenagy, H. S., Sparks, T. L., Ebben, C. J., Wooldrige, P. J., Lopez-Hilfiker, F. D., Lee, B. H., ... Cohen, R. C. (2018). NOx Lifetime and NOy Partitioning During WINTER. *J. Geophys. Res. Atmos.*, *123*(17), 9813–9827. doi: 10.1029/2018JD028736

Kiendler-Scharr, A., Mensah, A. A., Friese, E., Topping, D., Nemitz, E., Prevot, A. S., ... Wu, H. C. (2016). Ubiquity of organic nitrates from nighttime chemistry in the European submicron aerosol. *Geophys. Res. Lett.*, *43*(14), 7735–7744. doi: 10.1002/2016GL069239

Lee, A. K. Y., Adam, M. G., Liggio, J., Li, S.-M., Li, K., Willis, M. D., ... Brook, J. R. (2019). A Large Contribution of Anthropogenic Organo-Nitrates to Secondary Organic Aerosol in the Alberta Oil Sands. *Atmos. Chem. Phys. Discuss.*, 1–25. doi: 10.5194/acp-2018-1177

Lee, B. H., Mohr, C., Lopez-Hilfiker, F. D., Lutz, A., Hallquist, M., Lee, L., ... Thornton, J. A. (2016). Highly functionalized organic nitrates in the southeast United States: Contribution to secondary organic aerosol and reactive nitrogen budgets. *Proc. Natl. Acad. Sci.*, *113*(6), 1516–1521. Retrieved from `http://www.pnas.org/lookup/doi/10.1073/pnas.1508108113` doi: 10.1073/pnas.1508108113

Liebmann, J., Sobanski, N., Schuladen, J., Karu, E., Hellén, H., Hakola, H., ... Crowley, J. N. (2019). Alkyl nitrates in the boreal forest: Formation via the NO₃, OH and O₃ induced oxidation of BVOCs and ambient lifetimes. *Atmos. Chem. Phys. Discuss.*(3), 1–23. doi: 10.5194/acp-2019-463

Perring, A. E., Pusede, S. E., & Cohen, R. C. (2013, aug). An Observational Per-

spective on the Atmospheric Impacts of Alkyl and Multifunctional Nitrates on Ozone and Secondary Organic Aerosol. *Chem. Rev.*, *113*(8), 5848–5870. Retrieved from http://pubs.acs.org/doi/abs/10.1021/cr300520x doi: 10.1021/cr300520x

Pye, H. O., Luecken, D. J., Xu, L., Boyd, C. M., Ng, N. L., Baker, K. R., ... Shepson, P. B. (2015). Modeling the Current and Future Roles of Particulate Organic Nitrates in the Southeastern United States. *Environ. Sci. Technol.*, *49*(24), 14195–14203. doi: 10.1021/acs.est.5b03738

Ridley, B. A., Walega, J. G., Dye, J. E., & Grahek, F. E. (1994). Distributions of NO, NOx, NOy, and O3 to 12 km altitude during the summer monsoon season over New Mexico. *J. Geophys. Res. Atmos.*, *99*(D12), 25519–25534. Retrieved from http://dx.doi.org/10.1029/94JD02210 doi: 10.1029/94JD02210

Rollins, A. W., Browne, E. C., Min, K.-E., Pusede, S. E., Wooldridge, P. J., Gentner, D. R., ... Cohen, R. C. (2012). Evidence for NOx Control over Nighttime SOA Formation. *Science (80-.).*, *337*(6099), 1210–1212. Retrieved from http://science.sciencemag.org/content/sci/337/6099/1210.full.pdf doi: 10.1126/science.1221520

Romer Present, P. S., Zare, A., & Cohen, R. C. (2019). The changing role of organic nitrates in the removal and transport of NO_x. *Atmos. Chem. Phys. Discuss.*(x), 1–18. doi: 10.5194/acp-2019-471

Ryerson, T. B., Williams, E. J., & Fehsenfeld, F. C. (2000). An efficient photolysis system for fast-response NO2 measurements. *J. Geophys. Res. Atmos.*, *105*(D21), 26447–26461. doi: 10.1029/2000JD900389

Sobanski, N., Thieser, J., Schuladen, J., Sauvage, C., Song, W., Williams, J., ... Crowley, J. N. (2016). Day- and Night-time Formation of Organic Nitrates at a Forested Mountain-site in South West Germany. *Atmos. Chem. Phys. Discuss.*, 1–26. Retrieved from http://www.atmos-chem-phys-discuss.net/acp-2016-874/ doi: 10.5194/acp-2016-874

Starn, T. K., Shepson, P. B., Bertman, S. B., Riemer, D. D., Zika, R. G., & Olszyna, K. (1998). Nighttime isoprene chemistry at an urban-impacted forest site. *J. Geophys. Res. Atmos.*, *103*(D17), 22437–22447. doi: 10.1029/98JD01201

von Kuhlmann, R., Lawrence, M. G., Pöschl, U., & Crutzen, P. J. (2003). Sensitivities in global scale modeling of isoprene. *Atmos. Chem. Phys. Discuss.*, *3*(3), 3095–3134. doi: 10.5194/acpd-3-3095-2003

Xiong, F., McAvey, K. M., Pratt, K. A., Groff, C. J., Hostetler, M. A., Lipton, M. A., ... Shepson, P. B. (2015). Observation of isoprene hydroxynitrates in the Southeastern United States and implications for the fate of NOx. *Atmos. Chem. Phys. Discuss.*, *15*(13), 17843–17886. doi: 10.5194/acpd-15-17843-2015

Xu, L., Guo, H., Boyd, C. M., Klein, M., Bougiatioti, A., Cerully, K. M., ... Ng, N. L. (2015). Effects of anthropogenic emissions on aerosol formation from isoprene and monoterpenes in the southeastern United States. *Proc. Natl. Acad. Sci. U. S. A.*, *112*(1), 37–42. doi: 10.1073/pnas.1417609112

Xu, L., Suresh, S., Guo, H., Weber, R. J., & Ng, N. L. (2015). Aerosol characterization over the southeastern United States using high-resolution aerosol mass spectrometry: Spatial and seasonal variation of aerosol composition and sources with a focus on organic nitrates. *Atmos. Chem. Phys.*, *15*(13), 7307–7336. doi: 10.5194/acp-15-7307-2015